



Regular Article

Relationship between grain size and thermal hysteresis of martensitic transformations in Cu-based shape memory alloys



P. La Roca^{a,1}, L. Isola^a, Ph. Vermaut^{b,c}, J. Malarria^{a,*}

^aInstituto de Física Rosario (CONICET-Universidad Nacional de Rosario), Bvrd. 27 de Febrero 210 Bis, S2000EZF Rosario, Argentina

^bChimie ParisTech, PSL Research University, CNRS, Institut de Recherche de Chimie Paris (IRCP), Paris F-75005, France

^cSorbonne Universities, UPMC University Paris 06, UFR926, Paris 75005, France

ARTICLE INFO

Article history:

Received 24 December 2016

Received in revised form 15 February 2017

Accepted 11 March 2017

Keywords:

Shape memory alloys

Copper alloys

Martensitic phase transformation

Grain size

ABSTRACT

The effect of grain size on thermal hysteresis is studied in ribbons and thin strips obtained by rapid solidification techniques. Results show a strong increase of the hysteresis width when the grain size is below $\sim 100\mu\text{m}$. This effect is attributed to frictional work spent to accommodate the different martensitic variants in a zone close to grain boundaries, which constitutes an energy barrier proportional to the grain boundary area. A model for describing this effect based on thermodynamics and fitted experimental data is proposed.

© 2017 Acta Materialia Inc. Published by Elsevier Ltd. All rights reserved.

Shape-memory alloys (SMA) display unique and desirable thermomechanical properties, such as superelasticity, shape memory, and rubber-like behavior. These properties are related to the first-order displacive and diffusionless martensitic transformation between a metastable high-temperature phase and a low-temperature martensite phase, which has lower symmetry [1].

During this thermoelastic transformation, there is local equilibrium between three energies: the difference in chemical Gibbs free energy of the involved phases (i.e. between β and martensite phases like 18R or 2H); and the stored elastic energy (E^{Elas}); and the energy dissipated (E^{Fric}) by the frictional forces ($\Delta G^{\beta \rightarrow M} = E^{\text{Elas}} + E^{\text{Fric}}$) [2]. The frictional term, related to energy spent on overcoming resistance to the parent/martensite interface motion that is dissipated mainly as irreversible heat [3], is responsible for the thermal hysteresis and opposes the transformation during both the forward (FT) and the reverse transformation (RT).

During the past years, the study of “size effects” in SMA materials has aroused interest in the scientific community. These size effects can be a consequence of grain size reduction to improve the mechanical properties, since Cu-based SMA are usually prone to

brittle intergranular fracture [4], or by the length-scale reduction of different macro or microstructural characteristic in order to use these materials in small-scale devices [5–8].

Polycrystalline Cu-based shape memory materials with coarse grains, which undergo a martensitic transformation to a monoclinic 18R structure, display a hysteresis width similar to that of the single crystal (about 10 K). However, the thermal hysteresis increases when the grain size is reduced below $100\mu\text{m}$ [9,10]. Due to the close relationship between the thermal hysteresis and the stress hysteresis in a pseudoelastic cycle, the control of the martensitic transformation hysteresis is essential, even though the martensitic transition can be either thermally or stress-induced. This is quite important in actuator device design, where a small hysteresis is required for fast actuation applications [11–13]. In case of dampers, a hysteresis increase leads to possible enhanced energy dissipation (i.e. damping capacity). This enhanced damping capacity is useful for many practical applications [14]. Such behavior was observed, for instances, in bulk polycrystalline Cu-Al-Be alloys, where the pseudoelastic stress hysteresis increases as the grain size decreases [15,16]. A similar size effect was found in Cu-Al-Ni microwires, where the thermal and stress hysteresis increase as wire diameter decreases. This is particularly noticeable for wires with a diameter smaller than $100\mu\text{m}$ [17]. At a finer length scale, San Juan et al. [18] reported higher energy dissipation in Cu-Al-Ni submicron pillars than in bulk specimens of the same composition, showing a damping-capacity dependence on the pillar size, in the submicron range.

* Corresponding author at: IFIR, 27 de Febrero 210 bis, Rosario 2000, Argentina.
E-mail address: malarria@ifir-conicet.gov.ar (J. Malarria).

¹ Present address: Centro Atómico Bariloche, Comisión Nacional de Energía Atómica (CNEA) and Instituto Balseiro (UNCuyo), Av. Ezequiel Bustillo 9500, 8400 S. C. de Bariloche, Argentina.

Table 1
Casting parameters.

Ribbon/strip	Alloy [at.%]	Method	v_r [m/s]	T_{melt} [K]	d (as-cast) [μm]
R1	Cu-13 Al-5 Ni	MS	19	1640	10 ± 4
R2	Cu-13 Al-5.5 Ni-1 Ti	MS	19	1660	2.1 ± 1.0
R3	Cu-12 Al-0.5 Be	MS	15	1550	12 ± 5
S1	Cu-13 Al-5 Ni	TRC	0.6	1440	24 ± 10
S2	Cu-13 Al-6 Ni-1 Ti	TRC	0.84	1420	6 ± 3

Although many authors have observed the grain size dependence of martensitic transformation temperatures [14,19–23] and systematic analyzed it [24], until now the effect of grain size on the hysteresis width has not been studied over a wide range of grain sizes.

In Cu-based SMA, if the grain size is modified by changing annealing conditions after cold work, the annealing can alter the dislocation structure, and in addition, martensite nuclei can be trapped in dislocation tangles. This complicates any investigation of how grain size affects hysteresis and transformation temperatures. We overcome this issue through our material fabrication process. In this work, Cu-based ribbons and strips were obtained by rapid solidification methods of melt spinning and twin-roll casting. Fine grained specimens with a narrow spread in grain size were obtained, nearly free of dislocations within the grains. The experimental measurements are fitted assuming that the energy barrier produced by microplasticity and dissipative processes is proportional to the grain surface area. We discuss the validity of this hypothesis in the present scenario.

Melt spinning (MS) and twin-roll casting (TRC) are suitable techniques to develop SMA Cu-based materials with columnar grains with sizes ranging between 500 nm and 30 μm in section [25–28]. In this work, ribbons and sheets 50 μm and 300 μm thick were obtained by MS and TRC respectively. Processing parameters, alloy compositions and grain sizes are listed in Table 1.

The specimen's compositions were selected in order to obtain a single transformation from the parent phase to the 18R martensite structure [29,30]. In order to perform a study over a wide grain-size range, the samples received thermal treatments at 973 K, 1073 K and 1173 K for 30 min, followed by ice-water quenching. An additional thermal treatment at 473 K for 15 min followed by air cooling was performed, to promote ordering and to eliminate excess vacancies in the as-cast and thermally treated samples [31].

The microstructures were examined using an Olympus PME3 optical microscope (OM), a FEI Quanta 200 scanning electron microscopy (SEM) with Field Emission Gun and a FEI TECNAI F20 transmission electron microscopy (TEM). The grain sizes were determined using optical and TEM images, assuming a circular shape for the grain sections and averaging the diameter measurements for different grains. The standard deviation was taken as a measure of uncertainty.

The martensitic transformation was characterized by differential scanning calorimetry (DSC) and electrical resistivity measurements. DSC measurements were performed using a Shimadzu Differential Scanning Calorimeter DSC60, at 5 K/min, while the electrical resistivity behavior was characterized by the four-probe technique in AC mode, using a generic function generator and SR-530 Lock-in amplifier. At least three runs for the forward and reverse transformations were performed to verify reproducibility of the DSC and resistivity curves.

It should be noted that a small quantity of Ti was added to the R2 and S2 samples, in order to reduce the grain size in the Cu-Al-Ni alloys [32] by the precipitation of $(\text{CuNi})_2\text{TiAl}$ or CuNiTiAl (X phase), which are Heusler-type compounds with an $L2_1$ ordered structure. Two kinds of precipitates are observed and designated X_L or X_S ,

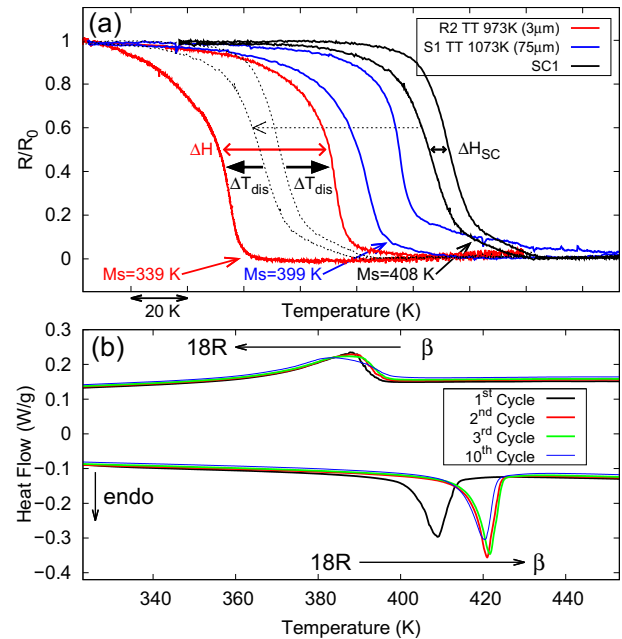


Fig. 1. Resistivity vs. temperature behavior for a single-crystal and samples with different grain sizes (a) and successive DSC curves for the R1 sample (as-cast condition) (b).

depending on size and distribution. On the one hand, the X_L precipitate size is about 500 nm and they are located at the grain boundaries. Therefore, their interactions with the martensitic transformation is not very significant. On the other hand, the X_S precipitates are only tens of nanometers in size and are located inside the grains as well as at the grain boundaries. A high density of X_S coherent precipitates leads to a change of the hysteresis width [33]. In order to avoid this effect, all samples with Ti were thermally treated above 973 K during 30 min, to ensure that the precipitates were the X_L -type [33]. Finally, as a reference, a 3 mm diameter Cu-13Al-5Ni single crystal, designated SC1, was included in the present analysis.

Fig. 1 (a) shows resistivity versus temperature curves for the single crystal and two samples with different grain sizes, which undergo a martensitic transformation to the monoclinic 18R structure. Cu-based single crystals display a hysteresis of about 10 K. However, when the grain size decreases the hysteresis becomes wider. In particular, the sample with a grain size of $2.9 \pm 1.3 \mu\text{m}$ shows a hysteresis of 42 ± 5 K, which is four times greater than that of the single crystal. DSC curves of the R1 sample (as-cast condition) are displayed in Fig. 1 (b). The curves settle down to those shown in Fig. 1 (b) for the second cycle, and no significant changes are observed in a first stage of cycling. A slight evolution became noticeable after 10 cycles. A first cycle effect in Cu-based SMA is a well known phenomena [34] that take place when the end of the reverse transformation A_f interferes with the temperature range where thermally activated processes become considerable. This allows residual stresses and excess of vacancies introduced after quenching to be eliminated. Therefore, the values of hysteresis width were determined from the 3rd thermal cycle of each sample.

The hysteresis as a function of grain size (d) is shown in Fig. 2 (a). This figure contains the experimental results of the hysteresis measurements performed by DSC and resistivity techniques on the MS and TRC samples. The uncertainty in hysteresis width was estimated from the maximum discrepancy between measurements in samples with the same grain sizes, using the resistivity and DSC techniques. This hysteresis width uncertainty is only plotted on a point, as a reference. In order to complete these data, the values for MS

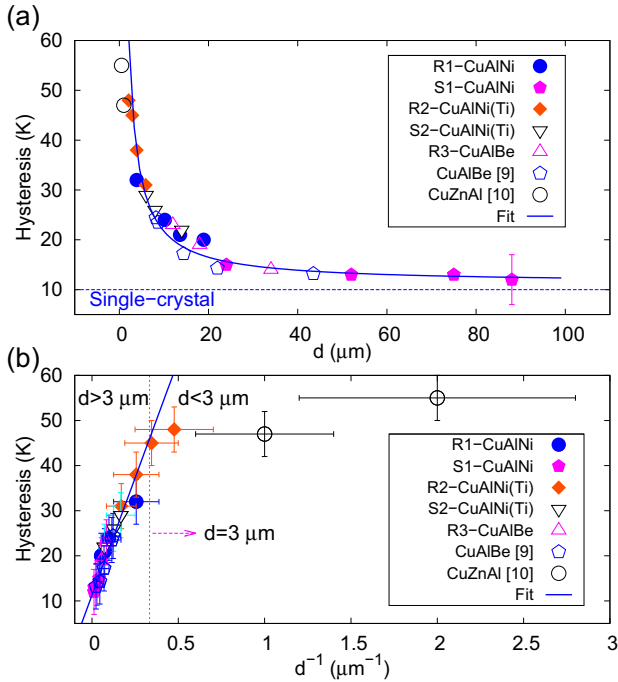


Fig. 2. Hysteresis as a function of d (a) and as a function of d^{-1} (b).

samples of Ref. [9] and of thin films obtained by sputtering [10] are included. Clearly the hysteresis width increases as d decreases, and its for $d > 100 \mu\text{m}$ the value is close to that of the single crystal.

In the thermodynamic framework of the martensitic transformation, the dissipative process derived from grain boundary constraint introduces an additional energy barrier (W^{dis-gb}), which must be overcome to proceed with the transformation. This energy barrier can be assumed to be proportional to the grain-boundary area.

In order to quantify the energy barrier, a cylindrical shape is assumed for the grains, since most of the values plotted in Fig. 2 correspond to samples with columnar grain structure. Then, the additional energy per unit volume is given by the following expression:

$$W^{dis-gb} = \gamma^{dis} \frac{A(d)}{V(d)} = \frac{\gamma^{dis} \cdot 4}{d} \quad (1)$$

where $V(d)$ and $A(d)$ are the volume and the boundary area of the cylindrical grain, while γ^{dis} is the dissipative energy per unit grain area. Note that in Eq. (1), it was used the cylinder side area ($A(d) = \pi d h$, where h is the cylinder height), since this represents the grain boundaries of the columnar grains. Also, it is necessary to stress that same grain size dependence would be obtained if spherical grain shape were assumed ($W^{dis-gb} = \gamma^{dis} \frac{A(d)}{V(d)} = \frac{\gamma^{dis} \cdot 6}{d}$) and the following deduction and the ensuing discussion could be performed to equiaxial grains.

To fit the experimental measurements shown in Fig. 2, it is necessary to relate this energy barrier to the hysteresis width increase. The dissipative effects yield a positive and negative transformation temperature shift in FT (ΔT_{dis}^{FT}) and RT (ΔT_{dis}^{RT}) respectively, in comparison to the single-crystal transformation temperature (see Fig. 1). As a first approximation, these transformation temperature shifts shall be assumed equal ($\Delta T_{dis} = \Delta T_{dis}^{FT} = \Delta T_{dis}^{RT}$). Then, the relation between the energy barrier and ΔT_{dis} is evaluated as [35]:

$$W^{dis-gb} = -\Delta S \cdot \Delta T_{dis} = \frac{\gamma^{dis} \cdot 4}{d} \quad (2)$$

where $\Delta S = -2 \times 10^5 \text{J/m}^3\text{K}$, which is the entropy change between the two phases [3,36]. So, taking into account that the total hysteresis width (ΔH) is twice ΔT_{dis} plus the single-crystal hysteresis (ΔH_{sc}), the hysteresis as a function of the grain size is:

$$\Delta H = 2 \cdot \Delta T_{dis} + \Delta H_{sc} = \frac{\gamma^{dis} \cdot 8}{-\Delta S d} + \Delta H_{sc} \quad (3)$$

The experimental measurements were fitted by expression (3) using γ^{dis} and ΔH_{sc} as fitting parameters over the 3–100 μm grain size range and the results are shown in Fig. 2 (a) and (b), for $\Delta H_{sc} = 11.3 \pm 0.7 \text{K}$ and $\gamma^{dis} = 2.6 \pm 0.2 \text{J/m}^2$. The independent term (ΔH_{sc}) is in good agreement with the hysteresis usually reported for $\beta \rightarrow 18R$ martensitic transformations in single crystals [1,37,38]. The proper fit of experimental data by Eq. (3) supports the concept that the energy barrier produced by dissipative effects is proportional to the grain-boundary area. In Fig. 2 (b) ΔH is plotted as a function of d^{-1} . A linear relationship fits well the experimental results for $d > 3 \mu\text{m}$ where the model captures the hysteresis behavior. By displaying data in this way, a discrepancy between the proposed function and the experimental values can be clearly noted for $d < 3 \mu\text{m}$. Note that the proposed function predicts very large hysteresis width values for a grain size $< 1 \mu\text{m}$. These large values disagree with the hysteresis width of $55 \pm 2 \text{K}$ measured by Haberkorn et al. [10], in thin films with an average grain size of about $500 \pm 200 \text{nm}$. The limit of the proposed approach will be discussed later in connection with microstructural images. It should be mentioned here that Lara-Rodriguez et al. [9] suggested that the thermal hysteresis decreases linearly with $d^{-1/2}$ for Cu-Al-Be ribbons produced by melt spinning (their data are included in Fig. 2 (a) and (b)). However, this result should be regarded as an approximate tendency, since it was obtained from a limited number of data measured over a narrow range of grain sizes.

So, as noted, the hysteresis width vs. grain size behavior reasonably follows a d^{-1} dependence for samples with grain sizes above 3 μm . In addition the ΔH_{sc} value aligns well with experimental values of the single-crystal hysteresis. However, it remains to be seen if the obtained dissipative energy γ^{dis} is physically reasonable.

In order to get a better insight into the origin of the dissipative effects responsible for the hysteresis, a TEM study was conducted to see how thermal cycling affects alloy's microstructure. Fig. 3 (a) is a TEM image of the R3 sample in the as cast state ($d \sim 10 \mu\text{m}$), where a low dislocation density near grain boundaries can be observed. These are "thermal" dislocations produced during the rapid-solidification process, and they are scanty and evenly dispersed within the microstructure. However, when the sample undergoes just about a few thermal cycles, the dislocation density increases at the grain boundary environment (see Fig. 3 (b) and (c)). The presence of some scarce microplates of martensite retained in dislocations tangles close to the grain boundaries (Fig. 3 (b) and (c)) is also notable. The grain boundaries strongly alter the microstructure of shape memory alloys since they constitute strong barriers to the propagation of martensite plates. This leads to different martensite structures near the boundaries, creating strong enough stress fields to generate dislocation slip and to retain martensite plates. These microstructural changes are not observed in single crystals after such a rather low number of cycles [39].

These TEM observations reflect the microplasticity activity produced by the martensitic transformation in a zone on both sides of the grain boundaries, which can be called the "Microplasticity Affected Zone" (MAZ). It originates from the interaction of moving interfaces with grain boundaries [40], and it can occur whenever self-accommodation is hindered [41]. Thus, the increase in hysteresis width should be regarded as the frictional work that take place in the MAZ. That is, the accommodation of variants in the neighborhood of the grain boundaries requires nonconservative movement of

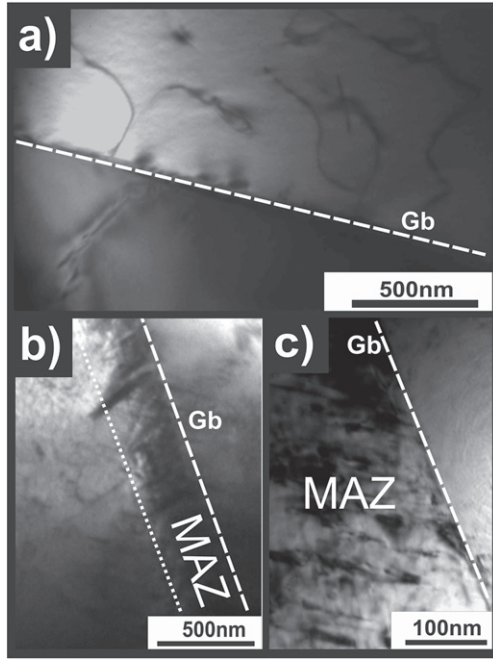


Fig. 3. TEM bright field image of R3 sample: (a) as-cast state, (b) and (c) after 10 thermal cycles where dislocations and some martensite plates are observed in the neighborhood of the grain boundaries.

material, which leads to an energy dissipation much higher than is seen in single crystals.

DSC curves presented in Fig. 1 (b) show that between the second and the tenth cycle the shift of the transformation temperatures is <2 K. Clearly, at this stage, cycling has no important effect on the hysteresis value. On the other hand, the dislocations accumulated around the grain boundaries after 10 thermal cycles revealed by TEM observations allows us to delineate the extent of the MAZ.

From the analysis of many samples, the averaged width of this MAZ is estimated at about $d_m = 300$ nm (Fig. 3 (b) and (c) are representative of the microstructure usually observed). Then, the effective volume involved in energy dissipation, resulting from the interaction of moving interfaces with the MAZ, can be quantified. This allows us to assess the energy dissipated per unit volume ($E_{V_{MAZ}}^{dis}$), in addition to the dissipative “background” already present in well-annealed single crystalline specimens, or in this case, in the zone inside the grains where the self-accommodation of martensite variants is in principle not hindered. This energy is assessed from γ^{dis} (the dissipative energy per unit area of the grain boundary), taking into account that the MAZ volume is proportional to the grain boundary area, as follows:

$$E_{V_{MAZ}}^{dis} = \frac{\gamma^{dis} A}{V_{MAZ}} \approx \frac{\gamma^{dis}}{d_m} = 8.6 \times 10^6 \text{ J/m}^3 \quad (4)$$

where V_{MAZ} is the MAZ volume.

It is important to stress that the width of defect zone near to grain boundaries is not regular and changes for different grains, and no correlation with the grain size could be established. Then the obtained $E_{V_{MAZ}}^{dis}$ value is approximate and must be regarded as result of a rough guess. With this remark in mind, to assess if this value is physically reasonable, we can compare our results with those from other situations where microplasticity takes place in localized zones of the microstructure as a result of interaction of moving interfaces with defects or other restrictions for the growth or self accommodation of martensite variants. For instance, we can look the behavior of pseudoelastically cycled Cu-Zn-Al single-crystals, although, in this

case the hysteresis is created by a different process. During pseudoelastic cycling at low temperatures, bands are formed by a high density of dislocations and martensite plates retained in their stress fields [42]. The bands are evenly distributed across the material and lie mainly parallel to the basal plane of the martensite structure. They act as severe obstacles to the propagating martensite plates, just as the grain boundaries in a polycrystal, and the area around the defects constitutes the MAZ in this case. The stress-strain transformation curves show a strong increase in the area enclosed by the hysteresis loop, which is correlated with the density of dislocations tangles acting as obstacles. The difference between the hysteresis area after a high number of cycles (at a saturation stage) and that corresponding to the first cycle gives a value of $E_V^{dis} = 1.4 \times 10^6 \text{ J/m}^3$.

Another interesting example is the extra-heat dissipated in mixed $\beta \rightarrow 18R + 2H$ transformation in Cu-Al-Ni and Cu-Zn-Al-Mn alloys [43] where the simultaneous growth of two types of martensite lead to incomplete accommodation. The extra-heat dissipated in this case is ascribed to plastic deformation, where exothermic process take place, produced when interfaces of different types of martensite impinge on each other. It was estimated at about $4 \times 10^6 \text{ J/m}^3$ analyzing chemical and no-chemical energy contributions determined by DSC by Recarte et. al [3].

Although we compared with experiments performed in different scenarios, we seek to stand out here that our estimate of the energy per unit volume dissipated by interaction between the martensitic transformation and the MAZ ($E_{V_{MAZ}}^{dis}$) is of the same order of magnitude as the energy per unit volume dissipated in situations where microplasticity take place in localized zones of the microstructure. This agreement provide support to the proposed nature of the dissipative effects for the current experiments.

Finally, the extent of the grain-size range, over which the model is applicable deserves some consideration. As previously noted, the fitting function predicts a very large hysteresis width for grain sizes below $1 \mu\text{m}$. Thus, the model overestimates measurements performed on specimens with grain size below this value [10,44]. This disagreement between the model and measurements can be understood when length scales in the microstructure are considered. The present model considers a MAZ width between 100 nm and 500 nm, which is comparable with the average grain size of the materials studied. The concept of an energy barrier produced by dissipative effects proportional to the grain boundary area is valid when the grain size is at least one order of magnitude greater than the measured MAZ width. Hence, the correlation between hysteresis width and grain size is properly described by Eq. (3) for specimens with a grain size above $3 \mu\text{m}$. Below this limit, other mechanisms should be considered, which are beyond the scope of the present analysis.

Summarizing, the grain size effect on the thermal hysteresis width was studied over a large range of grain sizes and a strong was observed. Using the concept that the energy barrier produced by dissipative effects is proportional to the grain boundary area, a function with a d^{-1} dependence on hysteresis and two free parameters was successfully applied to fit the experimental measurements over a grain-size range between $3 \mu\text{m}$ and $100 \mu\text{m}$. The free parameters obtained by fitting the data give $\Delta H_{sc} = 11.3 \pm 0.7$ K and $\gamma^{dis} = 2.6 \pm 0.2 \text{ J/m}^2$. ΔH_{sc} corresponds to the asymptotic behavior, when grain-size effects are negligible, and matches well with the experimental value observed in single crystals for the $\beta \rightarrow 18R$ transformation. The comparison with experiments where the martensitic transformation involve some degree of microplasticity in localized regions indicates the feasibility of interpreting the value $\gamma^{dis} = 2.6 \pm 0.2 \text{ J/m}^2$ as dissipative energy per unit grain area resulting from frictional work (dissipated as heat). Dissipation occurs when martensite interfaces meet the grain boundaries. Evidence of microplasticity was observed in an environment of 100 nm–500 nm around the boundary limit.

Acknowledgement

The authors would like to thank Daniel Castelani for his valuable collaborations in the development and implementation of the instrumentation used in these experiments. We gratefully acknowledge financial support from the “Agencia Nacional de Promoción Científica y Tecnológica” (under grants PICT 2140 and PICT 3140) and the Argentine-French ECOS program (project A10E02).

References

- [1] K. Otsuka, C.M. Wayman, Cambridge University Press, Cambridge, 1998.
- [2] P. Wollants, J.R. Roos, L. Delaey, *Prog. Mater. Sci.* 37 (1993) 227–288.
- [3] V. Recarte, J.I. Pérez-Landazábal, P.P. Rodríguez, E.H. Bocanegra, M. Nó, J. San Juan, *Acta Mater.* 52 (2004) 3941–3948. <http://dx.doi.org/10.1016/j.actamat.2004.05.009>.
- [4] R.D. Dar, H. Yan, Y. Chen, *Scr. Mater.* 115 (2016) 113–117. <http://dx.doi.org/10.1016/j.scriptamat.2016.01.014>.
- [5] M. Kohl, A. Agarwal, V. Chernenko, M. Ohtsuka, K. Seemann, *Mater. Sci. Eng. A* 438–440 (2006) 940–943. <http://linkinghub.elsevier.com/retrieve/pii/S0921509306005843>. <http://dx.doi.org/10.1016/j.msea.2006.02.062>.
- [6] M. Tomozawa, H. Kim, a. Yamamoto, S. Hiromoto, S. Miyazaki, *Acta Mater.* 58 (2010) 6064–6071. <http://linkinghub.elsevier.com/retrieve/pii/S1359645410004581>. <http://dx.doi.org/10.1016/j.actamat.2010.07.024>.
- [7] J. Barth, B. Krevet, M. Kohl, *Smart Mater. Struct.* 19 (2010) <http://stacks.iop.org/0964-1726/19/i=9/a=094004?key=crossref.65a768925fb956b68b11086ae04388dc>. <http://dx.doi.org/10.1088/0964-1726/19/9/094004>.
- [8] N. Tuncer, C.A. Schuh, *Scr. Mater.* 117 (2016) 46–50. <http://dx.doi.org/10.1016/j.scriptamat.2016.02.011>.
- [9] G.A. Lara-rodriguez, G. Gonzalez, H. Flores-Zú niga, J. Cortés-pérez, *Mater. Charact.* 57 (2006) 154–159. <http://dx.doi.org/10.1016/j.matchar.2005.12.017>.
- [10] N. Haberkorn, F.C. Lovey, A.M. Condó, J. Guimpel, *Mater. Sci. Eng. B* 170 (2010) 5–8. <http://linkinghub.elsevier.com/retrieve/pii/S0921510710000784>. <http://dx.doi.org/10.1016/j.mseb.2010.01.058>.
- [11] J. Mohd Jani, M. Leary, A. Subic, M.A. Gibson, *Mater. Des.* 56 (2014) 1078–1113. <http://linkinghub.elsevier.com/retrieve/pii/S0261306913011345>. <http://dx.doi.org/10.1016/j.matdes.2013.11.084>.
- [12] A. Nespoli, S. Besseghini, S. Pittaccio, E. Villa, S. Viscuso, *Sens. Actuators, A* 158 (2010) 149–160. <http://dx.doi.org/10.1016/j.sna.2009.12.020>.
- [13] A. Evrigen, I. Karaman, R. Santamarta, J. Pons, C. Hayrettin, R. Noebe, *Acta Mater.* 121 (2016) 374–383. <http://linkinghub.elsevier.com/retrieve/pii/S1359645416306541>. <http://dx.doi.org/10.1016/j.actamat.2016.08.065>.
- [14] W.U. Jianxin, J. Bohong, T. Hsu, *Acta Metall.* 36 (1988) 1521–1526. [http://dx.doi.org/10.1016/0001-6160\(88\)90219-2](http://dx.doi.org/10.1016/0001-6160(88)90219-2).
- [15] S. Montecinos, A. Cuniberti, A. Sepúlveda, *Mater. Charact.* 59 (2008) 117–123. <http://dx.doi.org/10.1016/j.matchar.2006.11.009>.
- [16] M. Sade, F. de Castro Bubani, F.C. Lovey, V. Torra, *Mater. Sci. Eng. A* 609 (2014) 300–309. <http://dx.doi.org/10.1016/j.msea.2014.05.018>.
- [17] Y. Chen, C.A. Schuh, *Acta Mater.* 59 (2011) 537–553. <http://dx.doi.org/10.1016/j.actamat.2010.09.057>.
- [18] J.M. San Juan, M. Nó, J. Alloys Compd. (2011) 12–16. <http://linkinghub.elsevier.com/retrieve/pii/S0925838811020792>. <http://dx.doi.org/10.1016/j.jallcom.2011.10.110>.
- [19] P. La Roca, L. Isola, P. Vermaut, J. Malarria, *Appl. Phys. Lett.* 106 (2015) 221903. <http://dx.doi.org/10.1063/1.4922195>.
- [20] P. La Roca, L. Isola, P. Vermaut, J. a. Malarria, *Proc. Math. Sci.* 8 (2015) 1133–1139. <http://linkinghub.elsevier.com/retrieve/pii/S2211812815001789>. <http://dx.doi.org/10.1016/j.mspro.2015.04.177>.
- [21] K. Mukunthan, L. Brown, *Metall. Trans. A.* 11 (1989) 90505. [http://dx.doi.org/10.1016/0142-1123\(89\)90505-7](http://dx.doi.org/10.1016/0142-1123(89)90505-7).
- [22] C. López del Castillo, B. Mellor, M. Blázquez, C. Gómez, *Scr. Metall.* 21 (1987)
- [23] D.N. Adnyana, *Metallography* 19 (1986)
- [24] P. La Roca, L.M. Isola, C.E. Sobrero, P. Vermaut, J.A. Malarria, *Mater. Today Proc.* 2 (2015) S743–S746. <http://dx.doi.org/10.1016/j.matpr.2015.07.389>.
- [25] J. Dutkiewicz, T. Czeppe, J. Morgiel, *Mater. Sci. Eng. A* 275 (1999) 703–707.
- [26] J. Font, E. Cesari, J. Muntasell, J. Pons, *Mater. Sci. Eng. A* 354 (2003) 207–211. [http://dx.doi.org/10.1016/S0921-5093\(03\)00003-0](http://dx.doi.org/10.1016/S0921-5093(03)00003-0).
- [27] J. Malarria, C. Elgoyhen, P. Vermaut, P. Ochin, R. Portier, *Mater. Sci. Eng. A* 440 (2006) 763–767. <http://dx.doi.org/10.1016/j.msea.2006.02.122>.
- [28] C.E. Sobrero, R. Bolmaro, J. Malarria, P. Ochin, R. Portier, *Mater. Sci. Eng. A* 481–482 (2008) 688–692. <http://linkinghub.elsevier.com/retrieve/pii/S0921509307011707>. <http://dx.doi.org/10.1016/j.msea.2006.12.232>.
- [29] V. Recarte, R.B. Pérez-Sáez, E.H. Bocanegra, M.L. Nó, J.M. San Juan, *Mater. Sci. Eng. A* 275 (1999) 380–384.
- [30] S. Belkahl, G. Guenin, *J. Phys. IV* 1 (1991)
- [31] M. Somerday, R.J. Comstock, J.A. Wert, *Metall. Mater. Trans. A* 28 (1997) 2335–2341.
- [32] K. Adachi, K. Shoji, Y. Hamada, *ISIJ Int.* 29 (1989) 378–387.
- [33] I. Hurtado, P. Ratchev, J.V.A.N. Humbeeck, L. Delaey, *Acta Metall.* 44 (1996) 3299–3306.
- [34] E. Hornbogen, V. Mertinger, J. Spielfeld, *Scr. Mater.* 40 (1999) 1371–1375. <http://www.sciencedirect.com/science/article/pii/S1359646299000767>. [http://dx.doi.org/10.1016/S1359-6462\(99\)00076-7](http://dx.doi.org/10.1016/S1359-6462(99)00076-7).
- [35] J. Guimar aes, *Scr. Mater.* 57 (2007) 237–239. <http://linkinghub.elsevier.com/retrieve/pii/S1359646207002643>. <http://dx.doi.org/10.1016/j.scriptamat.2007.04.002>.
- [36] R. Romero, J.L. Pelegrina, *Mater. Sci.* 354 (2003) 243–250. [http://dx.doi.org/10.1016/S0921-5093\(03\)00013-3](http://dx.doi.org/10.1016/S0921-5093(03)00013-3).
- [37] M. Ahlers, *Prog. Mater. Sci.* 30 (1986) 135–186. [http://dx.doi.org/10.1016/0079-6425\(86\)90007-1](http://dx.doi.org/10.1016/0079-6425(86)90007-1).
- [38] A. Planes, L. Ma nosa, D. Ríos-Jara, J. Ortin, *Phys. Rev. B* 45 (1992) 7633–7639.
- [39] J. Pons, F.C. Lovey, E. Cesari, *Acta Metall. Mater.* 38 (1990) 2733–2740. [http://dx.doi.org/10.1016/0956-7151\(90\)90287-Q](http://dx.doi.org/10.1016/0956-7151(90)90287-Q).
- [40] S.M. Ueland, C.A. Schuh, *J. Appl. Phys.* 114 (2013) <http://dx.doi.org/10.1063/1.4817170>.
- [41] J.H. Yang, C.S. Zhang, L.C. Zhao, T.C. Lei, *Scr. Metall.* 21 (1987) 259–264.
- [42] J. Malarria, M. Sade, F.C. Lovey, *Z. Metallkd.* 87 (1996) 953–962.
- [43] C. Segui, E. Cesari, J. Van Humbeeck, *Mater. Trans. JIM* 31 (1990) 375–380.
- [44] M.J. Morán, A.M. Condó, F. Soldera, M. Sirena, N. Haberkorn, *Mater. Lett.* 184 (2016) 177–180. <http://dx.doi.org/10.1016/j.matlet.2016.08.027>.